Available online at www.sciencedirect.com
SCIENCE DIRECT®
Journal of Nuclear Materials 335 (2004) 77–82
journal of nuclear materials
www.elsevier.com/locate/jnucmat

Embrittlement of RAFM EUROFER97 by implanted hydrogen

C. Liu, H. Klein, P. Jung *

Institut für Festkörperforschung, Forschungszentrum Jülich, D-52425 Jülich, Germany

Received 21 April 2004; accepted 19 June 2004

Abstract

About 380 μm thick specimens of low-activation martensitic stainless steel EUROFER97 were homogeneously implanted with protons below about 70 °C to concentrations up to about 1200 appm. Tensile tests were performed at 25 and 200 °C. The tests at 25 °C showed an increase of yield stress and ultimate tensile strength and a decrease of uniform elongation and elongation to fracture, while effects at 200 °C were strongly reduced. Scanning electron microscopy showed virtually no change of the ductile, transgranular fracture mode by the implanted H. A slight decrease of necking was observed only at the highest concentrations. The results are compared to previous measurements on F82H-mod and to literature results on tensile tests after He implantation and neutron irradiation. F82H-mod specimens were also implanted under applied tensile stress to concentrations up to 1900 appm. Straining was ascribed to accumulation of atomic defects, but no fracturing occurred. Thermal desorption measurements are included on H-implanted and tensile tested F82H-mod specimens. The results show significant data scatter, even within one specimen, with the highest measured values being in accordance with the implanted amount. In general, the H content is decreased after testing at higher temperatures, but even after testing at 350 °C, some specimens contain significant amounts.
© 2004 Elsevier B.V. All rights reserved.

1. Introduction

Hydrogen and helium are the major transmutation products in materials under high-energy neutron irradiation. In addition, hydrogen may enter structural materials of a fusion reactor by implantation from the plasma or by diffusion from coolants or breeding materials (e.g. ^{3}H) [1]. Especially in materials with body-centred cubic structure, such as ferritic–martensitic steels, there are concerns about degradation of mechanical properties, e.g. hydrogen embrittlement, due to low solubility and high mobility of hydrogen isotopes. To simulate transmutation, hydrogen can be loaded into solids from gas phase or electrochemically. Another method is the implantation of energetic protons which avoids surface effects and improves the simulation of the transmutation process by simultaneous production of displacement defects. Therefore this technique was employed in the present study for the investigation of tensile property changes by hydrogen.

* Corresponding author. Tel.: +49 2461 614036; fax: +49 2461 614413.
E-mail address: p.jung@fz-juelich.de (P. Jung).

0022-3115/$ - see front matter © 2004 Elsevier B.V. All rights reserved.
doi:10.1016/j.jnucmat.2004.06.005

2. Experimental

2.1. Material

The reduced activation ferritic–martensitic steel EUROFER97 is used in the European fusion material programme as candidate structural material for application in the blanket of the next generation fusion devices (e.g. DEMO reactor). The major constituents of EUROFER97 (wt%) are: C: 0.11, N: 0.03, P: 0.005, V: 0.2, Cr: 9.0, Mn: 0.48, Fe: 89.0, Ni: 0.021, Nb: 0.0017, Ta: 0.07, W: 1.1. Sheets of about 400 μm thickness were cut from the steel plates by spark erosion and polished to thickness of 360–380 μm. This thickness was chosen as a compromise to reduce losses of hydrogen to the surfaces during implantation and on the other side to avoid excessively long implantation times. From the sheets, dog-bone shaped specimens were cut with 15 mm total length, 7.0×1.5 mm^2 gauge section, 1 mm fillet radii, and rectangular grips of 3 mm length and 5 mm width.

2.2. Implantation

Three specimens were soldered together on a copper heat sink by Wood's metal, limiting temperatures during implantation and un-mounting to less than 70 °C. The specimen holder was posed in a vacuum chamber behind a 25 mm Hastelloy window and a rotating degrader wheel with 51 Al foils. The beam energy behind the window was 12.5 MeV, giving a range of 390 μm in the steel, according to TRIM–SRIM code [2]. These calculations were also used to determine the thicknesses of the degrader foils (8–959 μm) for achieving homogeneous implantation with less than 1% inhomogeneity [3] throughout the specimens, and to determine the concurrently introduced displacement damage using a displacement energy of 40 eV [4] and a binding energy of 2 eV (Fig. 1). The calculated number of vacancies per implanted ion decreases from the front-side to the back-side of the specimens from about 38 to 14, giving an average of 28, corresponding to 3.6 at.% H/dpa. The implantation rate was typically 0.005 appm H/s, corresponding to 1.4×10^{-7} dpa/s. TRIM was used for better comparison with other irradiation environments, while dpa values lower by about a factor of two were estimated from resistivity measurements [5].

2.3. Implantation under stress

F82H-mod specimens were implanted with hydrogen at 125 °C under constant uniaxial stresses of 300 and 450 MPa, respectively, loaded by a spring. Specimens were cooled by flowing helium gas and the temperature was monitored by infrared pyrometry. Strain was measured by strain gauges, continuously during implantation and with higher precision during beam-off periods.

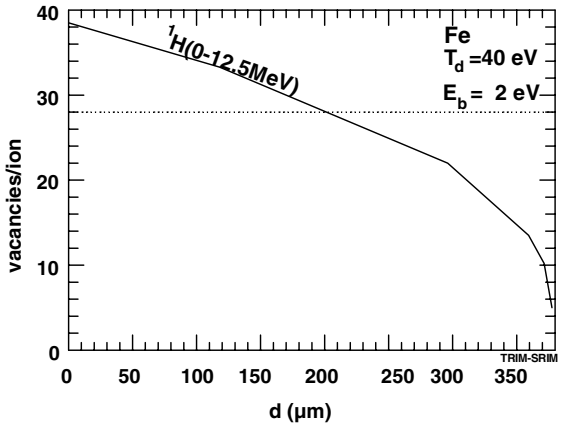

Fig. 1. Depth dependence of displacement damage produced by homogeneous implantation of protons of energies from 0 to 12.5 MeV in 380 μm iron ($\rho = 7.87$ g/cm^3, $T_d = 40$ eV, $E_b = 2$ eV), according to TRIM–SRIM calculations [2]. The dotted line gives the average value.

2.4. Tensile testing

The specimens were tensile-tested in a testing device for miniature specimens, located in a vacuum furnace under 10^{-3} Pa. Testing was started after evacuation and heating within about 0.5 h at a strain rate of 8.5×10^{-5}/s. Some tests with up to an order of magnitude higher strain rates showed no significant differences. Tensile tests were only performed at 25 and 200 °C, as the measurements already at 200 °C showed only a much lower effect of implanted hydrogen in agreement with previous measurements on F82H-mod. The latter experiments showed virtually no effect at 350 °C. Fracture surfaces were analysed by scanning electron microscopy (SEM) using a Hitachi S-4100 at a voltage of mostly 20 kV. The ratio of neck width w_{neck} to total thickness d of the foil specimens was used as a measure of the reduction of area A: $\Delta A/A = 1 - w_{neck}/d$.

2.5. Thermal desorption

After tensile testing, the hydrogen content of pieces of the specimens were analysed by thermal desorption spectroscopy. Up to four pieces were cut from the gauge section and analysed. The temperature was ramped linearly at 0.8 K/s from room temperature to about 1000 °C and the evolving hydrogen was determined by a quadrupole mass spectrometer under continuous pumping at constant pumping speed. Calibration of the spectrometer by three methods, namely a calibrated ion gauge, a controlled gas leak, and dissociation of TiH gave agreement within about 10%. Results are shown here for F82H-mod specimens from a previous implan-

tation and testing [6], because a larger number of specimens was available from this material.

3. Results

Fig. 2 gives tensile stress–strain curves before and after hydrogen implantation and tensile testing at 25 °C. The curves show a small but continuous increase of stresses and decrease of strains with increasing implantation dose, and reduction of work-hardening. Above yield stress, all specimens reveal some dynamic strain hardening. Yield stresses $\sigma_{0.2}$ and tensile stresses σ_{UTS} are summarised in Fig. 3, while Fig. 4 gives strains at ultimate tensile strength ε_{UTS} and total elongation at fracture ε_f, respectively. Fracture surfaces from SEM at all hydrogen implantation doses and testing temperatures gave no perceivable change of the transgranular, ductile, dimple-type fracture. Reduction of area ($1-w_{neck}/d$) shows only a drop at the highest dose for both testing temperatures (Fig. 5).

Results from implantation under stress are shown in Fig. 6. Straining tends at 300 MPa to level-off at values around 4×10^{-4}, while higher strains are reached at least by a factor of two at 450 MPa. No fracture appeared up to the highest concentrations.

Hydrogen desorbed from implanted (<70 °C) F82H-mod [6] during linear ramping of temperature in a broad single peak around 210 °C of typically 60 °C width (FWHM). The total released amount is compared to the implanted concentration in Fig. 7 with the temperatures of tensile testing indicated. The data show large scatter even for pieces from a single specimen. The dashed line would correspond to complete retention of the implanted hydrogen during implantation, unmounting and tensile testing. This large scatter of H content certainly is one reason for the scatter of mechanical data in Figs. 3–5.

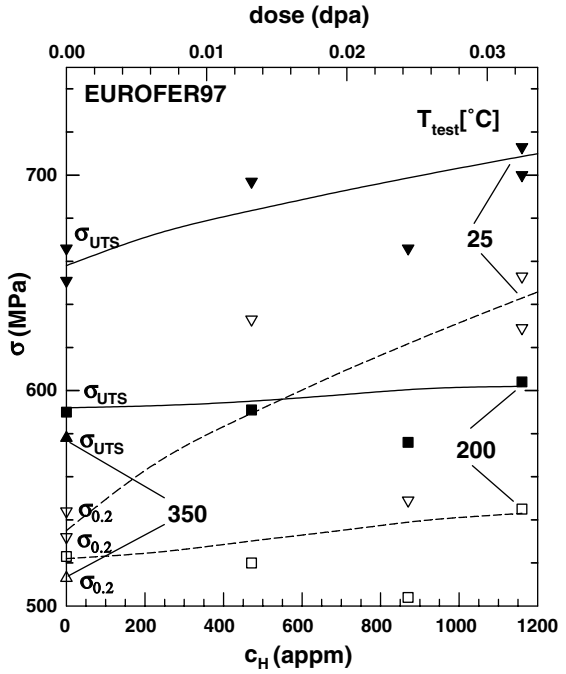

Fig. 3. Yield stress $\sigma_{0.2}$ and ultimate tensile stresses σ_{UTS} of 380 μm thick EUROFER97 specimens as a function of hydrogen concentration implanted below 70 °C and tested at 25 and 200 °C. The upper axis gives the average displacement dose as derived from Fig. 1. The dashed and solid lines give trends of $\sigma_{0.2}$ and σ_{UTS}, respectively, with the dashed line for 25 °C corresponding to Eq. (1) with parameters given in Table 1.

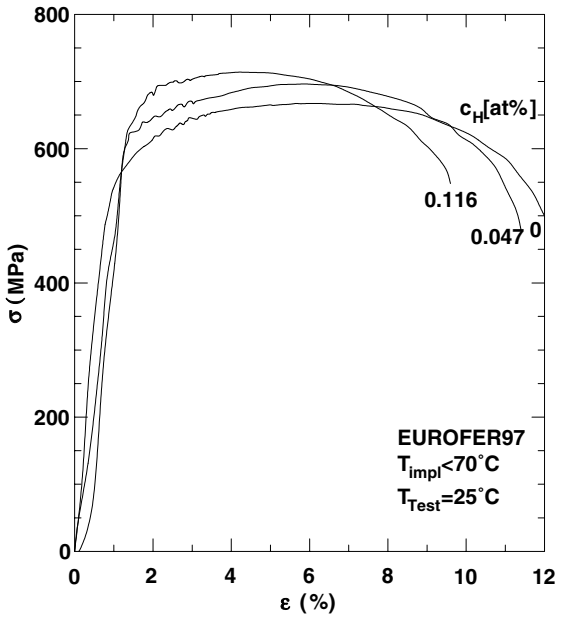

Fig. 2. Stress–strain curves of 365 μm thick EUROFER97 specimens after implantation below 70 °C to various H concentrations and testing at 25 °C at a strain rate of 8.5×10^{-5}/s.

4. Discussion

Comparison to previous studies on F82H-mod [6] shows that both $\sigma_{0.2}$ and σ_{UTS} of unimplanted EUROFER97 are significantly lower than the values of F82H-mod, with the differences decreasing from room temperature to 350 °C. On the other hand, EUROFER97 has a slightly higher uniform elongation ε_{UTS}, while ε_f values are similar. The tensile property changes of EUROFER97 after hydrogen implantation show similar behaviour as those of F82H-mod in previous measurements [6]. The dose dependence of the change of yield

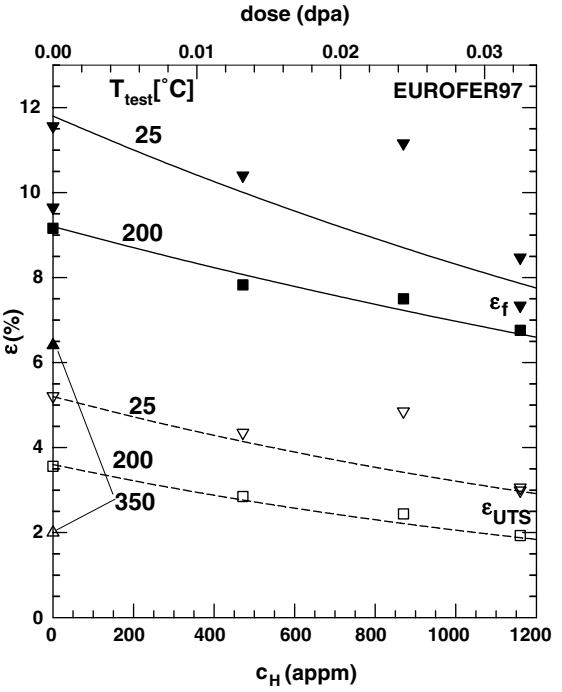

Fig. 4. Elongation at $\sigma_{UTS}(\varepsilon_{UTS})$ and total elongation ε_f of 380 μm thick EUROFER97 specimens as a function of implanted hydrogen concentration implanted below 70 °C and tested at 25 and 200 °C. The upper axis gives the average displacement dose as derived from Fig. 1. The dashed and solid lines give trends of ε_{UTS} and ε_f, respectively, with the dashed line for 25 °C corresponding to Eq. (2) with parameters given in Table 1.

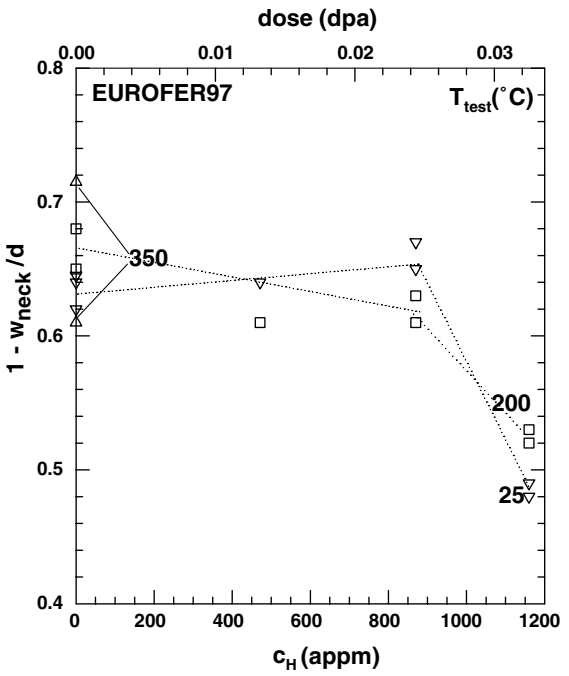

Fig. 5. Reduction of area 380 μm thick EUROFER97 specimens as derived from the ratio of neck width w_{neck} to total specimen thickness d.

stress of EUROFER97 after hydrogen implantation and subsequent tensile testing at 25 °C (Fig. 3) can be approximated by a power-law dependence on displacement dose Φ (see upper abscissa in Fig. 3) [7]:

$$\Delta\sigma_{0.2} = \sigma'(\Phi)^n. \quad (1)$$

Parameters σ' and n are listed in Table 1. Uniform elongation ε_{UTS} (Fig. 4) at low doses can be approximated by a logarithmic law:

$$\ln(\varepsilon_0/\varepsilon_{UTS}) = \Phi/\Phi' \quad (2)$$

with parameters $\varepsilon_0 = \varepsilon_{UTS}$ (0) and Φ' also given in Table 1. The strengthening coefficient n for hydrogen-implanted specimens of about 0.7 is in agreement with the behaviour of hardness of hydrogen-implanted F82H-mod and MANET-II which also shows a slightly higher than square-root dependence [8]. Exponents between 0.5 and 1 can be explained by superposition of hardening contributions from pre-existing dislocations and radiation-induced barriers, e.g. loops [9]. Results from EUROFER97 after He-implantation at 250 °C [9] and after neutron irradiation in HFIR [10] are included in Table 1. The remarkably uniform values of $n \approx 0.7 \pm 0.15$ and $\Phi' \approx 0.07 \pm 0.02$ after H and He implantation as well as after reactor irradiation show that hardening and loss of ductility in the very low dpa regime are dominated by displacement damage, with no specific effects of the implanted gases.

On the other hand, cathodically charged specimens show a strong drop of reduction of area at contents around 80 appm H when tested at room temperature, while testing at 100 and 200 °C give smaller but still distinct decreases at somewhat higher concentrations of around 200 appm H [11]. Irrespective of the fact that the $\Delta A/A$ values in Ref. [11] are much lower than the present results (Fig. 5), they indicate strong embrittlement by relatively low hydrogen concentrations, which is corroborated by other experiments on electrochemically loaded specimens (for a compilation see Ref. [1]). If this finding is combined with the results of the present work and of Ref. [6], one has to conclude that the irradiation induced defects, not withstanding the reduction of ductility by themselves, suppress embrittlement by hydrogen at low concentrations. A possible explanation would be trapping of hydrogen in irradiation-induced defects, e.g. vacancies, which could reduce its interaction with lattice defects or cracks. Such trapping was the subject of a recent investigation which will be reported elsewhere [12].

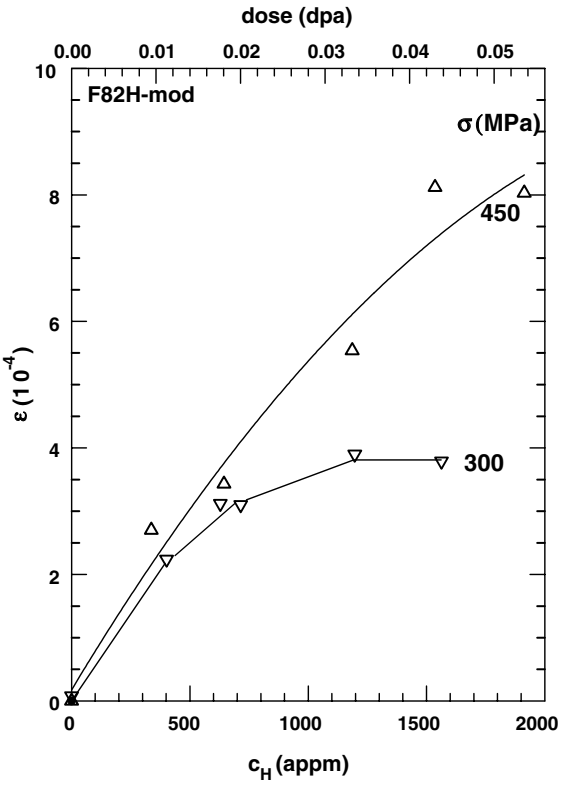

Fig. 6. Linear straining of 365 μm thick F82H-mod specimens during homogeneous implantation of hydrogen at 125 °C under stresses of 300 and 450 MPa. The symbols indicate measurements taken during beam-off periods at room temperature.

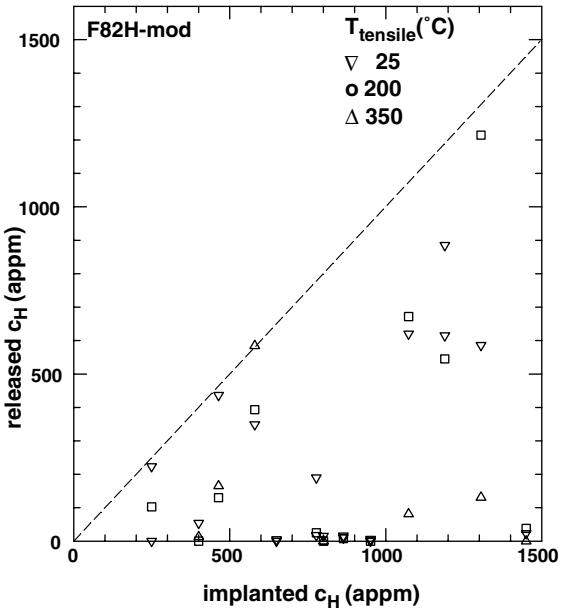

Fig. 7. Released versus implanted hydrogen concentration in 380 μm thick F82H-mod specimens as determined by desorption spectroscopy after tensile testing at the indicated temperatures.

The initial slope of the strain curves during implantation (Fig. 6) corresponds to a strain of 0.77 per unit concentration of implanted H. This is far above values from literature, which range from 0.114 [13] to 0.125 [14] for hydrogen in iron and steel. This indicates that most of the straining is due to the much higher concentration of irradiation defects produced simultaneously (28 defects/ion, see Section 2.2), part of which are surviving recombination. The levelling-off of the curves is ascribed to clustering of defects at higher concentrations, e.g. loop formation. It is generally supposed that the dilatational component of tensile stresses enhances hydrogen solubility, see Ref. [14], and therefore might increase embrittlement. The fact that this is not observed emphasises the importance of the opposing action of irradiation defects. In fact the tensile curves of F82H-mod after implantation under stress and testing at room temperature show similar behaviour as EUROFER97 in Fig. 2, i.e. enhanced strength and reduced ductility. Two peculiarities should be mentioned:

(1) The strong dynamic strain aging (similar to Fig. 2) of unimplanted F82H-mod disappears almost completely after implantation.
(2) The specimen implanted at 450 MPa features higher strength but has almost the same straining as unimplanted material. This means that its

Table 1
Comparison of the dependence of changes in yield stress $\Delta\sigma_{0.2}$ and ultimate tensile strain $\Delta\varepsilon_{UTS}$ on displacement dose Φ (dpa) for doses below about 0.05 dpa under various irradiation conditions

Material	Irradiation/Implantation	$T_{irr/impl}$ (°C)	T_{test} (°C)	$\Delta\sigma_{0.2} = \sigma'(\Phi)^n$		$\ln(\varepsilon_0/\varepsilon_{UTS}) = \Phi/\Phi'$		Ref.
				σ' (MPa)	n	ε_0 (%)	Φ' (dpa)	
EUROFER97	H-implantation	<70 °C	25	1460	0.76	5.2	0.058	This work
F82H-mod	H-implantation	<70 °C	30	2060	0.65	4.8	0.049	[6]
EUROFER97	He-implantation	250	25	1640	0.66	4.3	0.079	[9]
EUROFER97	He-implantation	250	250	1510	0.83	3.0	0.074	[9]
9Cr1MoVNb	Neutrons(HFIR)	60–100	25	1850	0.60	6.2	0.050	[10]

mechanical behaviour is virtually improved by implantation at the elevated temperature.

5. Summary and conclusions

- Yield stress and tensile strength increase and uniform and fracture strains decrease by implantation of hydrogen.
- At low doses these changes in tensile properties are comparable on the basis of atomic displacements to those after helium implantation and fast-neutron irradiation, and must therefore be mainly ascribed to displacement damage.
- Implanted hydrogen contents up to 0.12 at.% have no significant effect on the fracture mode.
- This indicates, in comparison to results after electrochemical loading, that embrittlement by hydrogen may be relieved under implantation/ irradiation conditions.
- Desorption measurements show large data scatter, but in some specimens noticeable amounts of hydrogen are retained even after testing at 350 °C. This scatter in H content certainly affects the results on mechanical properties.

References

[1] P. Jung, Fusion Technol. 33 (1998) 63.
[2] J.P. Biersack, L.G. Haggmark, Nucl. Instrum. and Meth. 174 (1980) 93;
J.F. Ziegler, Manual of TRIM Version 95.4, March 1995, unpublished.
[3] Z. He, P. Jung, Nucl. Instrum. and Meth. B 166&167 (2000) 165.
[4] P. Jung, Phys. Rev. B 23 (1981) 664.
[5] P. Jung, J. Nucl. Mater. 117 (1983) 70.
[6] P. Jung, C. Liu, J. Chen, J. Nucl. Mater. 296 (2001) 165.
[7] G.E. Lucas, J. Nucl. Mater. 206 (1993) 287.
[8] P. Jung, J. Nucl. Mater. 258–263 (1998) 124.
[9] P. Jung, J. Henry, J. Chen, J.-C. Brachet, J. Nucl. Mater., in press.
[10] K. Farrell, T.S. Byun, J. Nucl. Mater. 318 (2003) 274.
[11] A. Aiello, G. Benamati, L. Bertini, M.Beghini, ENEA, Report SM-A-R-001, (2003), unpublished.
[12] Z. Yao, C. Liu, P.Jung, in press.
[13] H. Hagi, Y. Hayashi, in: M.F. Ashby, J.P. Hirth (Eds.), Perspectives in Hydrogen in Metals, Pergamon, 1986, p. 141.
[14] J.O'M. Bockris, W. Beck, M.A. Genshaw, P.K. Subramanyan, F.S. Williams, Acta Metall. 19 (1970) 1209.